JBC RESEARCH ARTICLE

The secondary pocket of cryptochrome 2 is important for the regulation of its stability and localization

Received for publication, March 22, 2022, and in revised form, July 13, 2022 Published, Papers in Press, August 3, 2022,
https://doi.org/10.1016/j.jbc.2022.102334

Gizem Cagla Parlak[1,‡], **Bilge Bahar Camur**[1,‡], **Seref Gul**[2], **Onur Ozcan**[1], **Ibrahim Baris**[1], and **Ibrahim Halil Kavakli**[1,3,*]

From the [1]*Department of Molecular Biology and Genetics, Koc University, Istanbul, Turkey;* [2]*Biotechnology Division, Department of Biology, Istanbul University, Istanbul, Turkey;* [3]*Department of Chemical and Biological Engineering, Koc University, Istanbul, Turkey*

Edited by Brian Strahl

Human clock-gene variations contribute to the phenotypic differences observed in various behavioral and physiological processes, such as diurnal preference, sleep, metabolism, mood regulation, addiction, and fertility. However, little is known about the possible effects of identified variations at the molecular level. In this study, we performed a functional characterization at the cellular level of rare cryptochrome 2 (CRY2) missense variations that were identified from the Ensembl database. Our structural studies revealed that three variations (p.Pro123Leu, p.Asp406His, and p.Ser410Ile) are located at the rim of the secondary pocket of CRY2. We show that these variants were unable to repress CLOCK (circadian locomotor output cycles kaput)/BMAL1 (brain and muscle ARNT-like-1)–driven transcription in a cell-based reporter assay and had reduced affinity to CLOCK–BMAL1. Furthermore, our biochemical studies indicated that the variants were less stable than the WT CRY2, which could be rescued in the presence of period 2 (PER2), another core clock protein. Finally, we found that these variants were unable to properly localize to the nucleus and thereby were unable to rescue the circadian rhythm in a *Cry1*$^{-/-}$*Cry2*$^{-/-}$ double KO mouse embryonic fibroblast cell line. Collectively, our data suggest that the rim of the secondary pocket of CRY2 plays a significant role in its nuclear localization independently of PER2 and in the intact circadian rhythm at the cellular level.

The circadian clock is an endogenous timing system that controls physiological, metabolic, and behavioral processes over a 24 h period (1, 2). This rhythmicity is conserved from simple cyanobacteria to complex organisms and entrained by environmental cues, such as light, feeding, and social interactions (3, 4). The circadian timing system is mainly composed of a central pacemaker and a peripheral clock in mammals. The central pacemaker of the mammalian circadian clock is located in the suprachiasmatic nucleus and responsible for regulating and synchronizing peripheral clocks *via* neuronal and humoral signals (5).

The mammalian circadian clock is composed of interlocked transcriptional–translational feedback loops (TTFLs) at the molecular level. Transcriptional factors brain and muscle ARNT-like-1 (BMAL1) and circadian locomotor output cycles kaput (CLOCK) bind to E-box elements and initiate the transcription of clock-controlled genes including *Period* (*Per*) and *Cryptochrome* (*Cry*) by forming heterodimers, so they serve as the positive arm of the TTFL (5, 6). When phosphorylated by casein kinase Iδ/ε, PER–CRY heterodimers translocate into the nucleus and suppress CLOCK–BMAL1–mediated transcription (7). PERs and CRYs function as negative regulators of their own transcription and form the negative arm of the TTFL loop (8, 9). The ubiquitination of CRY and PER by F-box and leucine-rich repeat protein 3 (FBXL3) and β-transducin repeat–containing protein 1 (β-TrCP1), respectively, initiates proteasomal degradation of these proteins (10, 11). The repression on CLOCK–BMAL1 is relieved when CRY and PER are degraded, which resets the cycle (12).

Two mechanisms are proposed to explain the repression of the CLOCK–BMAL1–driven transcription by CRYs: blocking and displacement types of repression (13). The "blocking"-type repression takes place in the absence of PER where CRY1 interacts with the CLOCK–BMAL1 dimer on the E-box. Then, CRY1 represses the CLOCK–BMAL1 activity by inhibiting CLOCK–BMAL1 interaction with transcriptional machinery without removing them from the E-box (9, 14–16). The second type of repression mechanism, named "displacement"-type repression, takes place in the presence of PER2 where CRY1 causes dissociation of CLOCK–BMAL1 complex from the E-box (13). A biochemical study showed that PER2 alone cannot bind to CLOCK–BMAL1 heterodimer on DNA, and it requires the dissociation of CRY–CLOCK–BMAL1 from DNA (17). CKIδ within the PER–CRY–CKIδ complex phosphorylates CLOCK, which causes the release of CLOCK–BMAL1 by reducing their affinity to the E-box in a PER-dependent manner (18).

In mammals, two *Cry* genes are expressed, *Cry1* and *Cry2*, which belong to the photolyase/cryptochrome family (15). CRYs have two distinct domains: a photolyase homology (PHR) domain and an extended C-terminal domain (19, 20).

‡ These authors contributed equally to this work.
* For correspondence: Ibrahim Halil Kavakli, hkavakli@ku.edu.tr.

The role of the secondary pocket in CRY2 activity

The PHR domain of CRY is composed of two distinct domains called the primary (FAD-binding domain in photolyase) and secondary pockets (MTHF-binding domain in photolyase) (21). PHR and C-terminal domains of the CRYs are required to maintain the rhythmicity and amplitude of the circadian rhythm, respectively (22, 23). In addition, these domains are required for interacting with different proteins. For example, CRY1 interacts with the cystathionine β-synthase enzyme through its C-terminal end and regulates its activity (24), and with CLOCK and BMAL1 through two distinct regions on its PHR domain (25).

The secondary pockets of CRY1 and CRY2 are critical for the CLOCK binding and their repression activity (25). The accessibility of the secondary pocket is controlled by a serine loop, found in very close proximity to this pocket. Despite the high similarities between CRY1 and CRY2 sequences, subtle amino acid differences in the serine loop manage the loop dynamicity and, therefore, the differential binding affinity of CRYs to CLOCK (26). For instance, *in silico* mutation of only two amino acids on the serine loop of CRY2 to their corresponding amino acids in CRY1 (Ala61Gly and Ser64Asn) increased the dynamicity of the loop. Biochemical analysis showed that this double-mutant CRY2 had higher affinity to CLOCK–BMAL1 (26). In addition to the effect of serine loop composition on the dynamicity, it is allosterically regulated by the Arg-293 residue within the primary pocket in CRY1 (27). *In vitro* analysis showed that the p.Arg293His variant of CRY1 has a lower affinity to CLOCK–BMAL1 and produces a CRY2-like circadian phenotype in cell-based rescue assays. Further computational analysis revealed that there is no such allosteric regulation in CRY2 (28).

Disruption of the circadian clock through CRYs causes numerous behavioral and physiological diseases (1). Although the contribution of CRY mutations to disease progression is not well understood, several genetic studies have indicated that there is a relationship between CRY mutations and a variety of disorders such as advanced sleep phase, type 2 diabetes, familial delayed sleep phase disorder, attention deficit/hyperactivity disorder, and depression (29–33). For example, a rare SNP causing p.A260T mutation in CRY2 was shown to be associated with familial delayed sleep phase disorder. Molecular analysis showed that the p.Ala260Thr CRY2 variant cannot repress the CLOCK–BMAL1–driven transactivation, which is partly explained by the reduced stability and nuclear localization of the mutant CRY2 (29). Therefore, studies have been initiated to find small molecules against core clock proteins to regulate their activities and in turn to be used as therapeutics against CRY-related diseases (34–38).

Given the importance of the secondary pocket of CRYs in protein–protein interaction and the circadian clock mechanism, we selected three rare *Cry2* SNPs (p.Pro123Leu, p.Asp406His, and p.Ser410Ile) located within the secondary pocket rim to investigate their effects on the circadian rhythm at biochemical and cellular levels. Initially, we analyzed the repressor activity of the CRY2 variants on the CLOCK–BMAL1–dependent transactivation assay with and without overexpression of PER2 using cell-based *Per1*-d*luc* assay. All mutants had reduced repressor activity under all conditions. The CRY2 variants were less stable and had reduced affinity to CLOCK–BMAL1 complex compared with WT CRY2, but variants were able to restore their stability and affinity to CLOCK–BMAL1 complex when PER2 was overexpressed. To understand the effect of PER2 on CRY2 variants, nuclear fractionation analysis was carried out to probe the level of CRY2 at the subcellular level. The results revealed that CRY2 variants localize to the nucleus less than WT CRY2, independently of PER2 overexpression. To determine the effect of CRY2 variants on the circadian rhythm, we performed a complementation assay by transfecting plasmids consisting of the variants to a *Cry1*$^{-/-}$*Cry2*$^{-/-}$ mouse embryonic fibroblast (MEF) cell line in which none of the variants was able to rescue the circadian rhythm.

Collectively, our results suggest that the rim of the secondary pocket is important for the stabilization and translocation of the CRY2–PER2 complex to the nucleus and, in turn, its repressor activity.

Results

Selection of CRY2 variants

The database of the 1000 Genomes Project (39) and the Ensembl database (40) were used for the selection of human *C-RY2* variants. We used NM_021117.5 as a canonical mRNA transcript. A total of 380 missense variants in these databases were filtered based on the SIFT, PolyPhen, CADD, REVEL, MetaLR, and MutationAssessor scores. The selected variants are listed in Table 1. None of the variants is reported in the ClinVar database. Although the selected variants are not related to any disease according to the databases, MutationTaster predicted that all variants are "disease causing" (41). According to the American College of Medical Genetics and Genomics guideline, variants were classified as a "variant of uncertain significance" with two pathogenic criteria (PM2 and PP3) (42). *In silico* analyses (SIFT, PolyPhen, CADD, REVEL, MetaLR, and MutationAssessor) indicated that these variants may have negative effects on the structure and function of CRY2. The selected variants are either not detected or detected at a low frequency in gnomAD (gnomAD, version 2.1.1; https://gnomad.broadinstitute.org) (43–45). These findings indicate that each of them could be a potential disease-causing variant because of structural and functional changes in the protein (46, 47). Among those, p.Pro123Leu, p.Asp406His, and p.Ser410Ile variants (Fig. 1*A*), which are located on the rim of the secondary pocket of CRY2 that is highly conserved among different organisms (Fig. 1*B*), were selected to investigate their effects on CRY2–CLOCK binding and hence on circadian periodicity (48, 49).

Effect of CRY variants on CLOCK–BMAL1–driven transcription

The mutations (p.Pro123Leu, p.Asp406His, and p.Ser410Ile) were introduced into the complementary DNA (cDNA) of *Cry2* by site-directed mutagenesis (SDM). We then determined the repressor capacity of the CRY2 variants in a cell-based transactivation assay that has been widely used to

Table 1
The clinical features of CRY2 SNPs

Position in CDS (NM_021117.4)	Position in protein (NM_021117.4)	ACMG	gnomAD	ClinVar
c.86G>A	p.Arg29His	VUS (PM2, PP3)	Not detected	—
c.368C>T	p.Pro123Leu	VUS (PM2, PP3)	Not detected	—
c.484G>T	p.Gly162Trp	VUS (PM2, PP3)	Not detected	—
c.823C>T	p.Arg275Cys	VUS (PM2, PP3)	Not detected	—
c.833G>A	p.Cys278Tyr	VUS (PM2, PP3)	Not detected	—
c.838T>A	p.Ser280Thr	VUS (PM2, PP3)	Not detected	—
c.839C>G	p.Ser280Cys	VUS (PM2, PP3)	Not detected	—
c.848T>C	p.Leu283Pro	VUS (PM2, PP3)	Not detected	—
c.1074G>C	p.Trp358Cys	VUS (PM2, PP3)	Not detected	—
c.1138G>A	p.Val380Met	VUS (PM2, PP3)	f = 0.000003991	—
c.1139T>G	p.Val380Gly	VUS (PM2, PP3)	Not detected	—
c.1216G>C	p.Asp406His	VUS (PM2, PP3)	Not detected	—
c.1229G>T	p.Ser410Ile	VUS (PM2, PP3)	Not detected	—
c.1259C>T	p.Ser420Phe	VUS (PM2, PP3)	Not detected	—
c.1319G>A	p.Arg440His	VUS (PM2, PP3)	f = 0.000003991	—

Abbreviations: ACMG, American College of Medical Genetics and Genomics; CDS, coding sequence; VUS, variant of uncertain significance.

investigate protein–protein interactions among clock proteins (23, 27, 49–51). In this system, an E-box containing *Per1* promotor is fused with a destabilized luciferase gene (pGL3.1-*Per1*::d*Luc*) plasmid. Human embryonic kidney 293T (HEK293T) cells were transiently transfected with WT and variant pcDNA-*Cry2-His-Myc* plasmids (0.25, 0.5, 1, 2, 20, and 50 ng), where CRY2 was fused with His and Myc tag, along with plasmids consisting of the cDNA of *Bmal1*, *CLOCK*, and reporter pGL3.1-*Per1*::d*Luc*. All tested CRY2 variants showed reduced repressor activity on CLOCK–BMAL1 transactivation (Fig. 2*A*). To eliminate the possibility of problems with the variant expression in this assay, we checked their expression level by Western blot analysis. The protein extracts obtained from cells expressing these variants were subjected to SDS-PAGE followed by Western blot analysis using anti-Myc antibody to detect the level of CRY2. The three variants at low doses of plasmid (0.25, 0.5, 1, and 2 ng) had comparable expression compared with the WT CRY2 (Fig. 2*A*). However, three CRY2 variants had lower expression than WT CRY2 when high doses of *Cry2* plasmids (20 and 50 ng) were

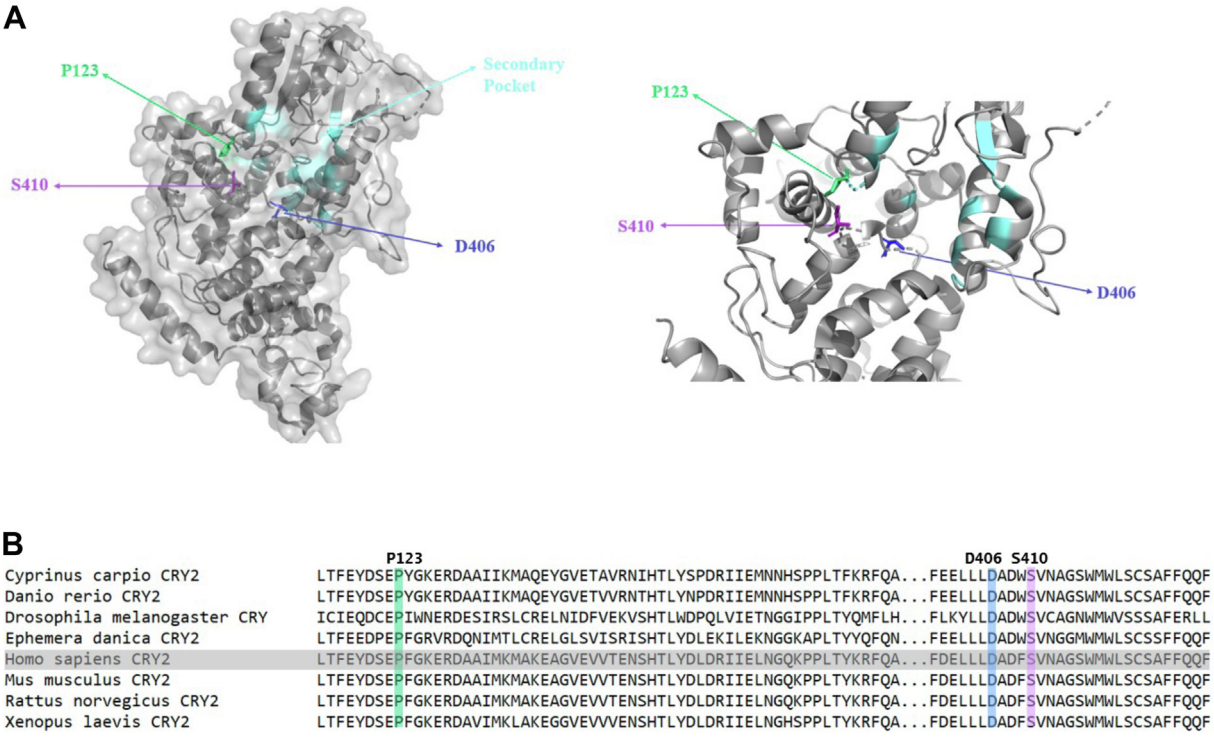

Figure 1. Visualization of SNP positions on the mouse CRY2 and multiple sequence alignment of CRY2 from different species. *A*, the mouse CRY2 (Protein Data Bank ID: 4I6E) structure is shown as a surface diagram, and the mutant residues are shown as a *stick*: P123 (*green*), D406 (*blue*), and S410 (*purple*). The CRY2 residues that generate the secondary pocket are colored *cyan*. The mCRY2 structure is shown as a *ribbon diagram*, and the mutant residues are shown as a *stick*: P123 (*green*), D406 (*blue*), and S410 (*purple*). The CRY2 residues that generate the secondary pocket are colored *cyan*. Figures were prepared using PyMol. *B*, multiple sequence alignment of selected CRY2 proteins. Human CRY2 is highlighted in *gray*, whereas residues Pro-123 (*green*), Asp-406 (*blue*), and Ser-410 (*purple*) are also shown. The protein accession numbers of the organisms are as follows: *Cyprinus carpio* (XP_018938637.1), *Danio rerio* (NP_571861.2), *Drosophila melanogaster* (AAF55649.1), *Ephemera danica* (KAF4523712.1), *Homo sapiens* (AAH41814.1), *Mus musculus* (AAD46561.1), *Rattus norvegicus* (NP_596896.2), and *Xenopus laevis* (NP_001082139.1). CRY2, cryptochrome 2.

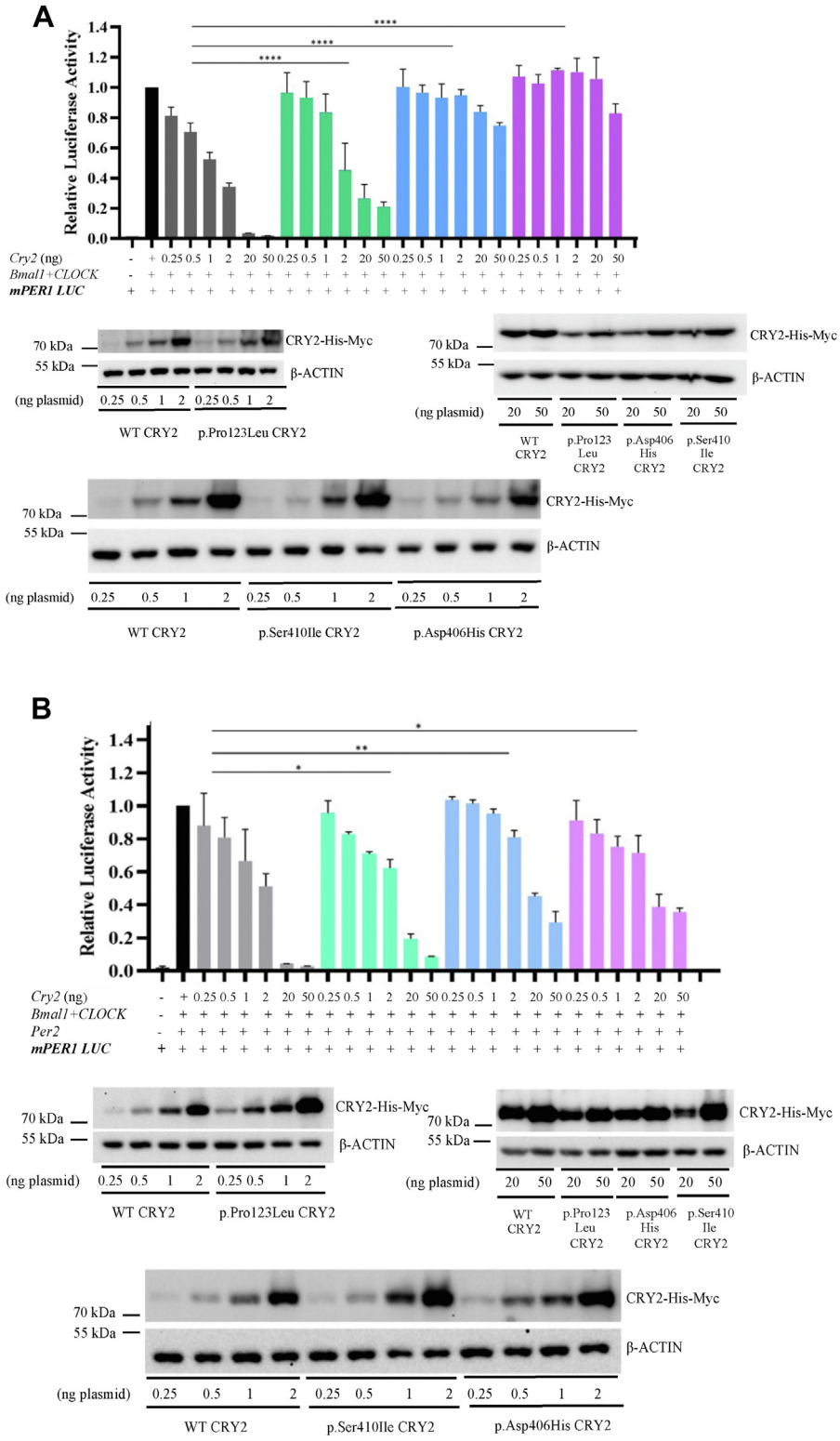

Figure 2. p.Pro123Leu CRY2, p.Asp406His CRY2, and p.Ser410Ile CRY2 variants have loss-of-function characteristics. *A*, dose-dependent repressor activity of WT CRY2 and p.Pro123Leu CRY2, p.Asp406His CRY2, and p.Ser410Ile CRY2 variants. WT CRY2 was used as a positive control. HEK293T cells were transfected with the indicated plasmids. Here, 0.25, 0.5, 1, 2, 20, and 50 ng of plasmids were used sequentially for each CRY2 variants. (Data represent the mean ± SEM, n ≥ 3 biological replicates with triplicate samples.) Significance analysis was performed using two-way ANOVA (****$p < 0.0001$). Comparisons were made between WT CRY2 and each mutant separately. Representative Western blot images of dose-dependent expression of WT CRY2 and p.Pro123Leu CRY2, p.Asp406His CRY2, and p.Ser410Ile CRY2 variants in the absence of overexpressed PER2. *B*, dose-dependent repressor activity of WT CRY2 and p.Pro123Leu CRY2, p.Asp406His CRY2, and p.Ser410Ile CRY2 variants in the presence of overexpressed PER2. WT CRY2 was used as a positive control. HEK293T cells were transfected with the indicated plasmids. Here, 0.25, 0.5, 1, 2, 20, and 50 ng of plasmids were used sequentially for each *Cry2*. (Data represent the mean ± SEM, n ≥ 3 biological replicates with triplicate samples.) Significance analysis was performed using two-way ANOVA (*$p < 0.05$; **$p < 0.005$). Comparisons were made between WT CRY2 and each mutant separately. Representative Western blot images of dose-dependent expression

transfected. Collectively, these results suggested that CRY2 variants have lower repressor activity, which may result from reduced stability of the variants and not from the low expression (quantification of blot is given in Fig. S1).

It has been shown that PER2 remodels the Ser loop of CRY2 and, in turn, regulates its repressor activity (52). Because the three variants are located at the rim of the secondary pocket, we investigated the repressor activity of the CRY2 variants in the presence of overexpressed PER2 with the *Per1*::d*Luc* assay on CLOCK–BMAL1–driven transcription (49). The results showed that PER2 partially rescued the repressor activity of the CRY2 variants (Fig. 2*B*). The p.Asp406His and p.Ser410Ile CRY2 variants were able to exhibit repressor activity to a certain degree under high doses of *Cry2* plasmids (2, 20, and 50 ng). Although p.Pro123Leu CRY2 variant exhibited some repressor activity on CLOCK–BMAL1 transactivation at all doses, PER2 was unable to rescue the repressor activity of the variant (Fig. 2*B*). Western blot analysis of protein extracts from these samples revealed that the CRY2 variants had comparable levels of the proteins compared with the WT (Fig. 2*B*, *below bar graph*).

Since the secondary pocket of CRYs is important for regulating the CLOCK–BMAL1 binding (25, 27, 49, 52), we then reasoned that the reduced repressor capacity of CRY2 variants is associated with the change in the affinity of the variants to CLOCK–BMAL1 complex, so they are unable to achieve proper repression. To address this, we carried out coimmunoprecipitation (co-IP) assays to determine the interaction between CRY2 variants and CLOCK–BMAL1 complex.

Investigation of the interaction between CRY2 variants and CLOCK–BMAL1 complex with and without overexpression of PER2

Plasmids consisting of *Bmal1*-FLAG, *CLOCK*-FLAG, and *Cry2*-His-Myc (or mutant *Cry2*-His-Myc) were transfected either with or without pSG-*Per2* plasmid to HEK293T cells. After preparing the extract from these cells, MYC resin was used to precipitate CRY2-His-Myc. The results indicated that WT CRY2 had a higher affinity to CLOCK when PER2 was overexpressed (Fig. 3), which is consistent with previous results (25, 27, 49, 52). Notably, the p.Pro123Leu and p.Ser410Ile CRY2 variants had a higher affinity to CLOCK when PER2 was overexpressed, whereas both variants had a greatly reduced affinity to CLOCK without PER2 overexpression (Fig. 3, *A* and *B*). Meanwhile, p.Asp406His CRY2 variant had a reduced affinity to CLOCK, which was recovered by the overexpression of PER2 (Fig. 3*C*). The affinity of either WT or p.Asp406His CRY2 variant to BMAL1 was comparable irrespective of the overexpression of PER2 (Fig. 3*C*). Co-IP analyses revealed that mutations in CRY2 diminished its CLOCK binding; however, overexpression of PER2 recovered the variant CRY2–CLOCK binding. To obtain insight into how CRY2 variants affect the interaction with PER2 and CLOCK, we performed co-IP studies between CRY2 variants and PER2 and CLOCK exclusively. Our results indicated that, compared with WT CRY2, all three variants had comparable interactions with PER2, whereas the variants' affinity to CLOCK was significantly reduced (Fig. 3*D*). These results indicate that the rim of the secondary pocket plays a role in CRY2–CLOCK binding.

Co-IP results showed that CRY2 variants had comparable affinity to CLOCK–BMAL1 complex in the presence of overexpressed PER2. We then reasoned that the reduced repressor activity of variants might be due to the change in their stability. We thus decided to investigate the half-life of the variants.

Stability of CRY2 variants

The stability of the CRY2 variants with and without the overexpression of PER2 was tested using cycloheximide (CHX) chase assay, as described previously (11, 53, 54). WT and variant *Cry2*-His-Myc plasmids (where *Cry2* was tagged with Myc at the C terminus) were transfected into HEK293T cells. Cells were grown overnight, treated with CHX, and then harvested 0, 4, 8, and 12 h later. The level of CRY2-Myc was determined using anti-Myc antibody. Analysis of the Western blot results revealed that, compared with WT CRY2, the p.Pro123Leu, p.Asp406His, and p.Ser410Ile CRY2 variants had reduced half-lives (Fig. 4*A*). Calculations indicated that $t_{1/2}$ of each variant CRY2 was decreased by approximately 70% (Fig. 4*A*). However, the overexpression of PER2 increased the stability of the CRY2 variants, and their half-lives became comparable to that of WT CRY2 (Fig. 4*B*).

We next investigated why CRY2 variants are less stable in the absence of PER2 overexpression. The degradation of CRYs is primarily driven by SCF^{FBXL3} and SCF^{FBXL21} (55–57). FBXL3 and FBXL21 have E3 ligase activity, but SCF^{FBXL21} ubiquitylates CRYs less efficiently than SCF^{FBXL3} (57, 58). Interestingly, while FBXL21 interacts with CRYs in both the cytoplasm and the nucleus, FBXL3 interacts entirely in the nucleus (55, 57). Thus, FBXL21 functions as the primary E3 ligase for CRY in the cytoplasm, whereas in the nucleus, it plays a protective role against FBXL3 (57). Therefore, we used MG132, an inhibitor of the proteasome complex, to investigate whether variants that are ubiquitylated by FBXL systems are being degraded through this complex. The results indicated that the blocking of the proteasome led to stabilization of WT and CRY2 variants, which suggests that the variants are still degraded through the proteasome complex (Fig. 5).

Effect of CRY2 variants on circadian rhythm at the cellular level

We next investigated the effect of CRY2 variants on the circadian rhythm using the MEF $Cry1^{-/-}Cry2^{-/-}$ (CRY-DKO MEF; double KO [DKO]) cell line developed by the Ueda group (59). Previous studies indicated that the *Cry2* gene in the

of WT CRY2 and p.Pro123Leu CRY2, p.Asp406His CRY2, and p.Ser410Ile CRY2 variants in the presence of overexpressed PER2. The WT CRY2 and variants were detected with anti-Myc. β-actin was used as a loading control. Since 20 and 50 ng of *Cry2* expression mask lower doses, they were represented in separate membranes. CRY2, cryptochrome 2; HEK293T, human embryonic kidney 293T cell line; PER2, period 2.

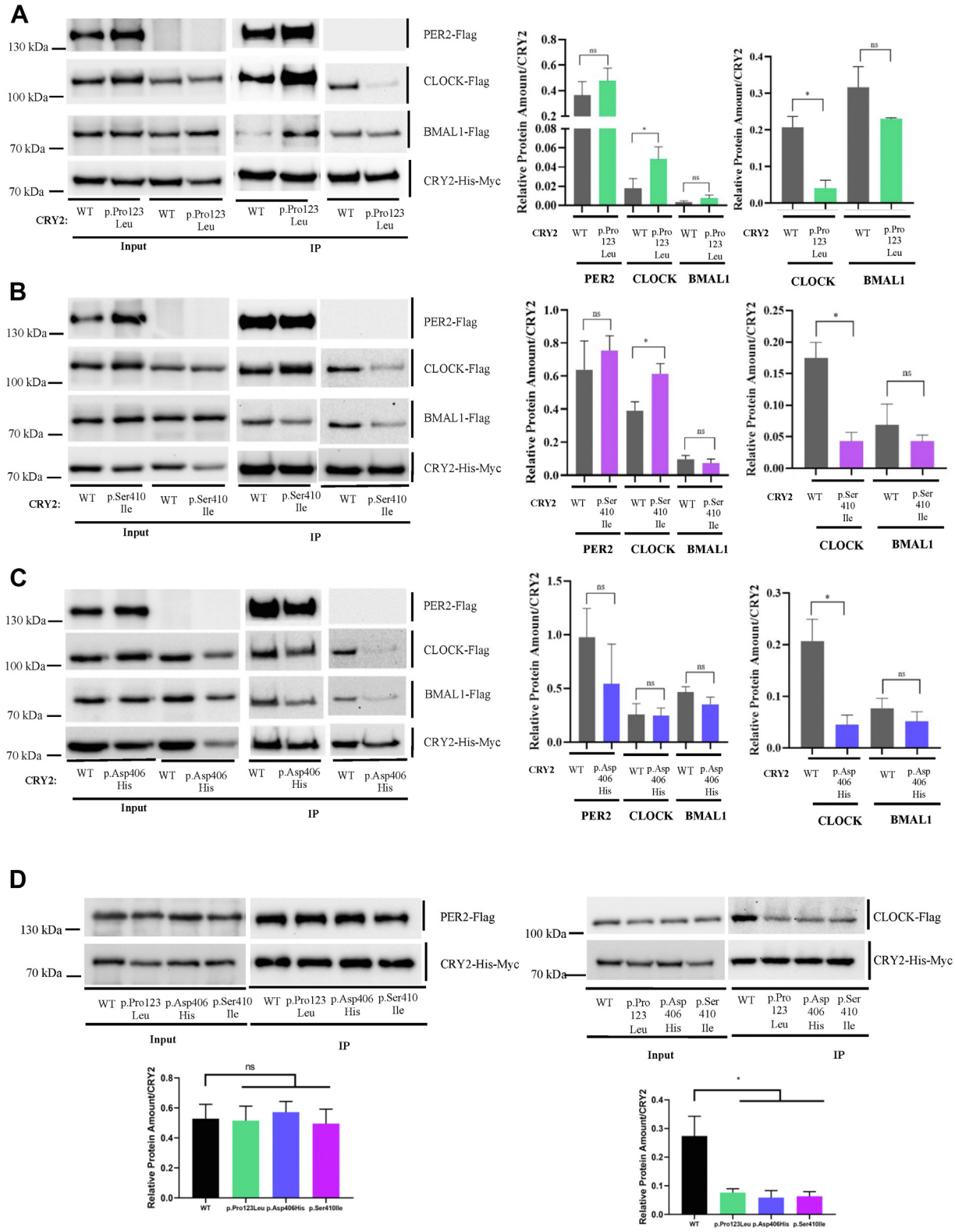

Figure 3. Determination of protein–protein interaction between CRY2 variants and CLOCK–BMAL1 complex in the absence and presence of PER2 overexpression. *A*, physical interaction between WT CRY2 and p.Pro123Leu CRY2 variant with CLOCK–BMAL1 and CLOCK–BMAL1–PER2. The blot shown is representative of three independent experiments. Quantification is given in the *bar graph*; a *gray* color represents the relative amount of WT CRY2, whereas a *green color* represents the relative amount of the p.Pro123Leu CRY2 variant. The *bar graph* in the *middle* shows the quantification of WT and CRY2 variants with overexpressed PER2. The *bar graph* on the *right* is the quantification of CRYs in the absence of PER2. *B*, physical interaction between WT and p.Ser410Ile CRY2 with CLOCK–BMAL1 and CLOCK–BMAL1–PER2. *Purple color* indicates the relative amount of p.Ser410Ile CRY2, and *gray color* indicates the relative amount of WT CRY2. *C*, physical interaction between WT and p.Asp406His CRY2 variant with CLOCK–BMAL1 and CLOCK–BMAL1–PER2. *Blue color* indicates the relative amount of the p.Asp406His CRY2 variant, and *gray color* indicates the relative amount of the WT CRY2. In all IP studies, HEK293T cells were transfected with plasmids expressing *Bmal1*-FLAG, *CLOCK*-FLAG, and WT or variant *Cry2*. Then, samples were pulled down with anti-MYC resin and analyzed

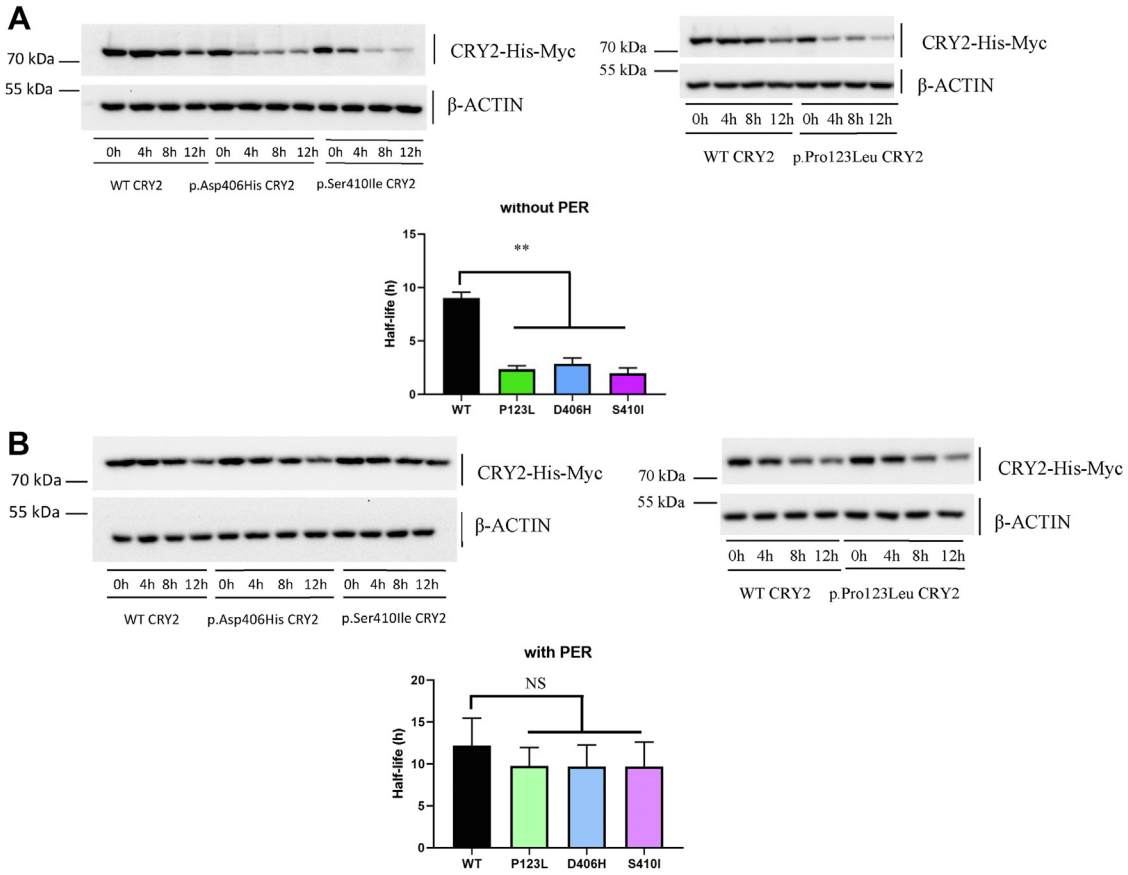

Figure 4. The CRY2 variants are less stable than the WT CRY2. *A*, representative Western blot images of protein degradation assay of WT CRY2 and p.Pro123Leu CRY2, p.Asp406His CRY2, and p.Ser410Ile CRY2 variants in the absence or *B*, the presence of overexpressed PER2. HEK293T cells were transfected with 500 ng of WT pcDNA4/myc-His-*Cry2* and variants and 500 ng of pFLAG-CMV-*Per2* (in *B*). The next day, 20 μg/ml CHX was used to stop protein expression. The WT CRY2 and variants were detected with anti-Myc. β-actin was used as a loading control. The half-lives of WT CRY2 and variants were calculated using a one-phase exponential decay function. Average $t_{1/2}$ values ± SEM from three independent experiments (n = 3). Significance analysis was performed using an unpaired *t* test with Welch's correction (**$p < 0.01$). Comparisons were made between WT CRY2 and variants. CHX, cycloheximide; CRY2, cryptochrome 2; HEK293T, human embryonic kidney 293T cell line; PER2, period 2.

pMU2 vector was able to rescue the circadian rhythm in CRY-DKO MEF (27, 49). We generated CRY2 variants using pMU2-*Cry2* plasmid by SDM. We then transfected *Cry2* variant plasmids along with pGL3-*Per2*-dLuc (luciferase reporter) to CRY-DKO MEF and placed them into the luminometer to monitor the circadian rhythm. As a control, WT pMU2-*Cry*1 or pMU2-*Cry2* plasmids with luciferase reporter were transfected into CRY-DKO MEF cells. As expected, cells expressing WT *Cry1* and *Cry2* rescued the circadian rhythm with long and short periods, respectively (Fig. 6). The CRY2 variants were unable to rescue the rhythm when 150 ng of plasmids were used (Fig. 6*A*). We then increased the amount of *Cry2* variant plasmids to 900 ng. However, CRY2 variants were still unable to rescue the rhythm (Fig. 6*B*).

Subcellular fractionation of the WT and variants of CRY2

Our findings suggested that variant CRY2s have comparable stability and expression levels when PER2 is overexpressed. It is therefore surprising to observe that CRY2 variants had defective CLOCK–BMAL1–mediated repression. The variants were unable to rescue the circadian rhythm even when a high dose of rescue plasmid was transfected. We then hypothesized that the localization of CRY2 variants might have been defective in the nucleus and thereby showed reduced repressor activity. To investigate this, we transfected plasmids coding WT and variants of CRY2 into HEK293T cells. Then, the cells were fractionated as described previously, in the absence or the presence of PER2 overexpression (24). The purity of cytosolic and nuclear fractions was assessed by Western blot using antitubulin and antihistone H3 antibodies (Fig. 7). The cytosolic levels of the three CRY2 variants were significantly lower than that of the WT CRY2 (Fig. 7*A*). Similarly, the level of the CRY2 variants was lower in the nucleus (Fig. 7*B*). This observation was attributed to the reduced stability of CRY2 variants. A similar study was performed with the overexpression of PER2. Although the levels of the CRY2 variants were similar to that of WT CRY2 in the cytosolic fraction

by Western blotting. All experiments were repeated three times (n = 3); significance analyses were performed using an unpaired *t* test with Welch's correction (*$p < 0.05$). BMAL1, brain and muscle ARNT-like-1; CLOCK, circadian locomotor output cycles kaput; CRY2, cryptochrome 2; HEK293T, human embryonic kidney 293T cell line; IP, immunoprecipitation; PER2, period 2.

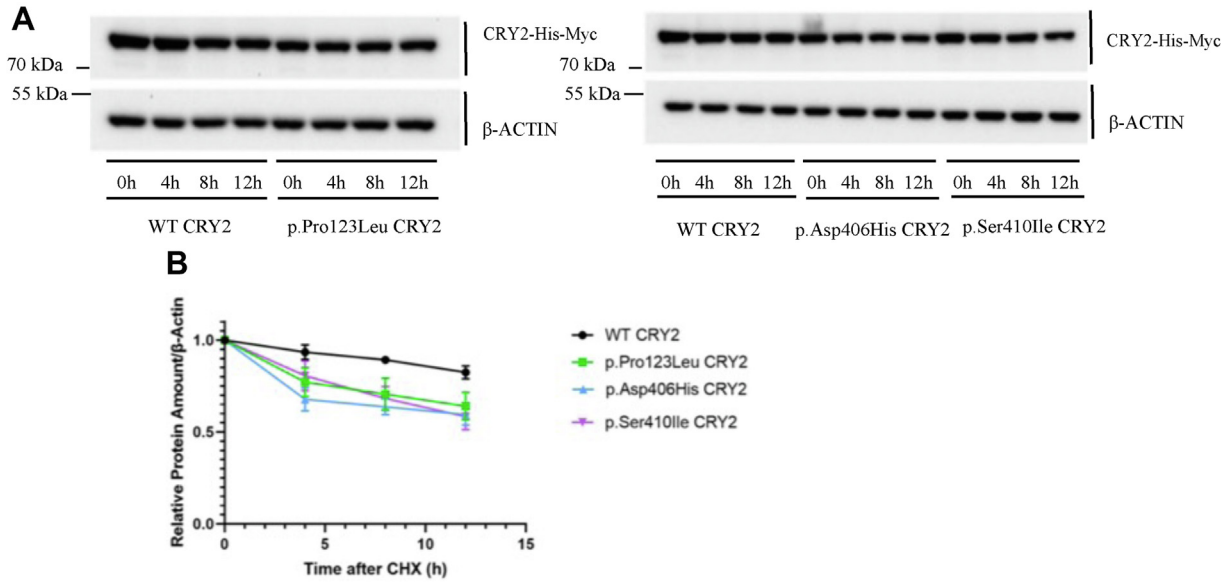

Figure 5. Stability of CRY2 variants is regulated through a proteasomal pathway. *A*, representative Western blot images of protein degradation assay of WT CRY2 and p.Pro123Leu CRY2, p.Asp406His CRY2, and p.Ser410Ile CRY2 variants in the presence of a proteasome inhibitor (MG132). HEK293T cells were transfected with 500 ng of WT *Cry2* and variants. The next day, 20 μg/ml CHX was used to stop protein expression and 10 μM MG132 was used to inhibit proteasome degradation. *B*, quantification of Western blots (n = 3). CRY2 amount of each variant or WT divided by β-actin and normalized according to the amount of CRY2 at *t* = 0 h. CHX, cycloheximide; CRY2, cryptochrome 2; HEK293T, human embryonic kidney 293T cell line.

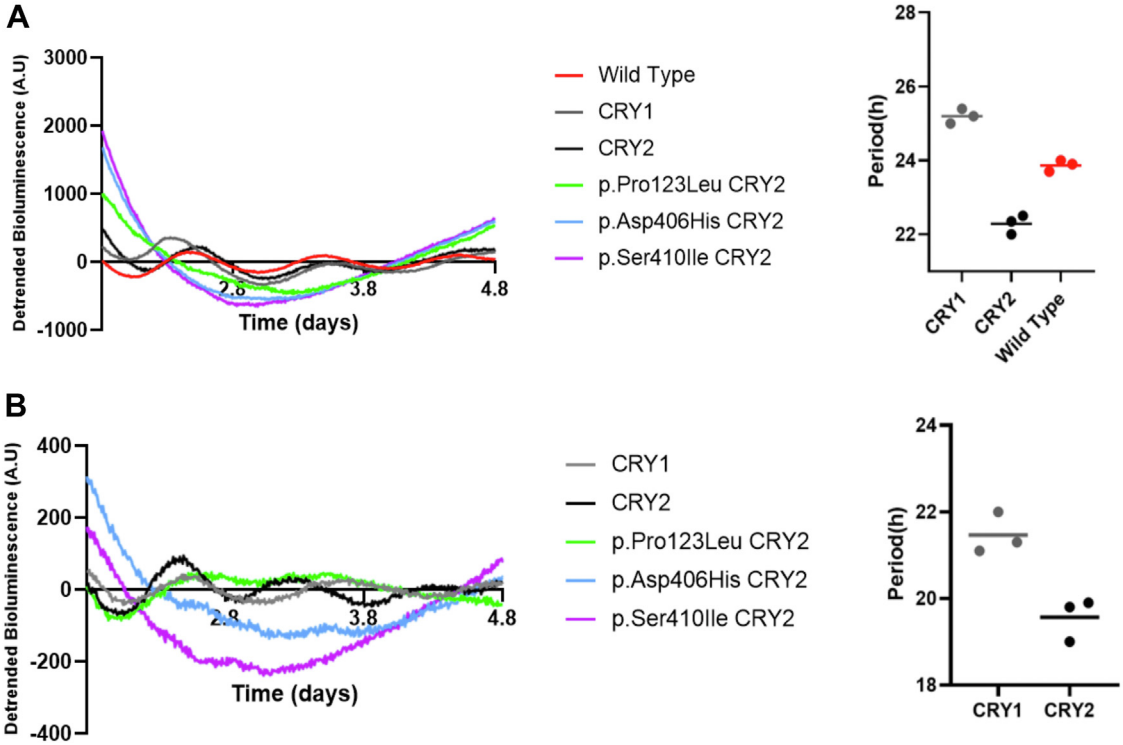

Figure 6. Complementation assay of the variants and WT CRY2. *A*, experiments were performed as described previously (59). The representative bioluminescence of three independent experiments (n = 3) is shown. CRY-DKO-MEF cells were transiently transfected with 4000 ng of pGL3-*Per2*-d*Luc* and 150 ng of WT *Cry2*, and *Cry1* and *Cry2* variants in rescue plasmids. After 72 h, cells were synchronized with dexamethasone, and luminescence values were recorded for 5 days. Period lengths of *Cry1* and *Cry2* rescued the rhythm in CRY-DKO cells. The periods of p.Pro123Leu CRY2, p.Asp406His CRY2, and p.Ser410Ile CRY2 variants could not be calculated because of the absence of rhythms. *B*, the representative bioluminescence of three independent experiments. DKO-MEF cells were transiently transfected with 4000 ng of pGL3-*Per2*-d*Luc* and 900 ng of WT *Cry2*, and *Cry1* and *Cry2* variants in rescue plasmids. After 72 h, cells were synchronized with dexamethasone and luminescence values were recorded for 5 days. Regarding period lengths of *Cry1* and *Cry2*, calculations were performed from three independent experiments (n = 3). Raw data were detrended by subtracting a least-squares fit of a second-degree polynomial and then mean centered. CRY2, cryptochrome 2; DKO, double KO; MEF, mouse embryonic fibroblast.

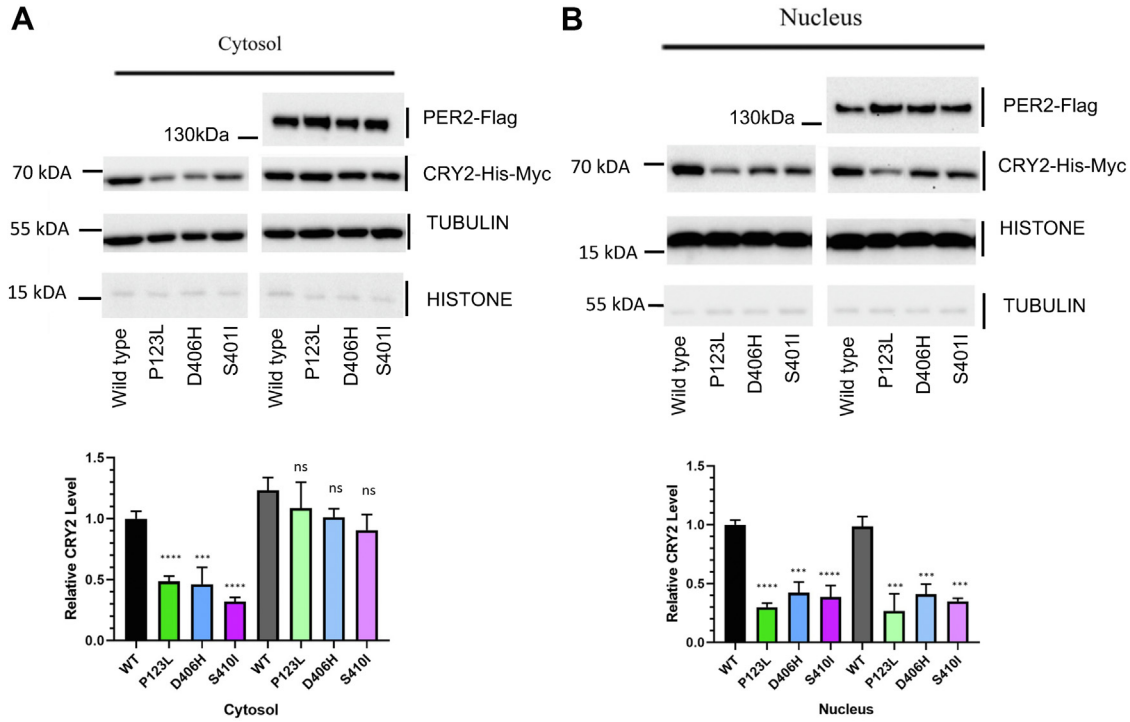

Figure 7. Subcellular localization of the WT and variants of the CRY2. HEK293T cells were transfected with 500 ng WT pcDNA4/myc-His-*Cry2* and variants and 500 ng pFLAG-CMV-*Per2*. The next day cells were harvested, and subcellular fractionation was performed. *A*, representative Western blot images and quantification of cytosolic fractions of WT CRY2 and p.Pro123Leu CRY2, p.Asp406His CRY2, and p.Ser410Ile CRY2 variants in the absence (*left*) and presence (*right*) of overexpressed PER2. The WT CRY2 and variants were detected with anti-Myc. Alpha-tubulin was used as control. Significance analysis was performed using unpaired *t* test (n = 3) (***$p < 0.0005$; ****$p < 0.0001$). Comparisons were made between WT CRY2 and each mutant separately. *B*, representative Western blot images and quantification of nuclear fractions of WT CRY2 and p.Pro123Leu CRY2, p.Asp406His CRY2, and p.Ser410Ile CRY2 variants in the absence (*left*) and presence (*right*) of overexpressed PER2. The WT CRY2 and variants were detected with anti-Myc. Histone H3 was used as control. Significance analysis was performed using unpaired *t* test (n = 3) (***$p < 0.0005$; ****$p < 0.0001$). Comparisons were made between WT CRY2 and each mutant separately. CRY2, cryptochrome 2; HEK293T, human embryonic kidney 293T cell line; PER2, period 2.

(Fig. 7*A*), the levels of the variants were significantly lower in the nuclear fraction than for WT CRY2 in PER2-overexpressed samples (Fig. 7*B*). The low levels of CRY2 variants in the nucleus, even upon the overexpression of PER2, can explain why the CRY2 variants were not able to repress CLOCK–BMAL1–driven transcription.

Discussion

Cryptochromes (CRYs) are potent transcription factors of the mammalian circadian clock and play a role in the negative feedback loop by repressing CLOCK–BMAL1 transactivation (1, 5, 7). The link between CRY mutations and various diseases has been shown in several genetic studies. A CRY2 variant (A260T), for example, causes advanced sleep phase in humans (29). The mutation changes the conformation of CRY2 and makes it more accessible to FBXL3 (an E3 ubiquitin ligase), which leads to its degradation. The same study also reported that p.Ala260Thr CRY2 mutation leads to lower CRY2 accumulation in the nucleus. Another study showed that type 2 diabetes and impaired fasting glucose are linked with another CRY2 variant (31). Moreover, a dominant CRY1 mutant (exon 11-deficient CRY1; CRY1 Δ11) was reported to be associated with delayed sleep phase disorder. This mutation causes a gain of function where CRY1 Δ11 is associated with enhanced affinity to CLOCK–BMAL1 (33). Another recent report showed that CRY1 exon 6 skipping mutation (CRY1 Δ6) is associated with attention deficit/hyperactivity disorder (32). Molecular and cell-based rescue assays showed that CLOCK binding to CRY1 Δ6 is completely diminished, and the rhythm cannot be rescued by the variant.

CRYs are composed of distinct domains, PHR domain and C-terminal domain, which are essential for CRYs' protein–protein interaction to maintain intact circadian rhythm in mammals. The PHR domain consists of an FAD-binding domain in photolyase (called the primary pocket) and an MTHF-binding domain in photolyase (called the secondary pocket). Mechanistic studies revealed that the secondary pocket accessibility of CRYs is regulated by the serine loop dynamicity, which is allosterically controlled in CRY1 (26–28). The amino acid compositions of CRY1 and CRY2 serine loops are the same except for two amino acids: Gly-43 and Asn-46 of CRY1 are replaced with Ala-61 and Ser-64 in CRY2. *In silico* mutations of these two amino acids of the CRY2 serine loop (A61G and S64N) caused a more flexible serine loop compared with that in WT CRY2 in molecular dynamics simulations (28), which can explain the different dynamicity of the serine loop in CRY1 and CRY2.

All these findings suggested that the secondary pocket of CRY2 is critical for intact CRY2 function, and CRY2 variants having mutation around the secondary pocket might affect the protein activity and the circadian rhythm. Therefore, in this

study, we selected rare genetic variants of *Cry2* (p.Pro123Leu, p.Asp406His, and p.Ser410Ile CRY2) from the Ensembl database, which are located on the rim of the secondary pocket, for molecular characterization (Fig. 1). None of these variants has been associated with diseases.

The repressor activity of the three CRY2 variants on CLOCK–BMAL1 transactivation was highly reduced (Fig. 2*A*). However, overexpression of PER2 partially restored their repressor activity, which may have been because of the protection of CRY2 from proteasomal degradation (Fig. 2*B*). This is supported by the CHX chasing assay, where the stabilities of the three variants were significantly lower than that of the WT CRY2 (Fig. 4*A*). However, the overexpression of PER2 in the same assay recovered the stability of the variants (Fig. 4*B*). It is known that there is competition between PER2 and FBXL3 for binding to CRY2 (11). The increased stoichiometry of PER2 during the assay might have reduced the affinity of CRY2 to FBXL3 and, in turn, increased the stability of the variants. Despite having more stable CRY2 variants in the presence of PER2, they were unable to repress CLOCK–BMAL1–driven transcription (Fig. 2*B*), which suggests that there might be a change in affinity between the CRY2 variants and CLOCK–BMAL1 complex. Co-IP analyses of the variants showed that the interaction of the CRY2 variants with CLOCK is significantly lower than that for WT CRY2, which is correlated with their reduced repressor activities (Fig. 3). Interestingly, overexpression of PER2 increased the affinity of CRY2 variants to CLOCK. Co-IP data indicated that amino acid residues at the rim of the secondary pocket are important for CLOCK binding and can be remodeled by PER2, although they are far away from the PER2-binding site (60).

To reveal the effect of CRY2 variants on the circadian rhythm, *Cry1*$^{-/-}$*Cry2*$^{-/-}$ MEF cells were transfected with rescue plasmids having mutant or WT *Cry2*. Cell-based rescue assay showed that none of the variants, even when high doses of plasmids were transfected, could rescue the rhythm (Fig. 6). Attenuated repression activity of CRY2 variants in the presence of PER2 overexpression and their inability to rescue the circadian rhythm in CRY-DKO cells may stem from the altered subcellular localization of the variants and thereby disrupt the negative arm of the TTFL. To explain the aforementioned observation, we further investigated the subcellular localization of the variants. Variants were unable to accumulate in the nucleus compared with WT CRY2, even upon the overexpression of PER2 (Fig. 7). This causes stochiometric changes in the core clock protein and, in turn, affects the circadian rhythm (35). A reduced level of the CRY2 variants in the nucleus and their low affinity for CLOCK may interfere with the displacement of the CLOCK–BMAL dimer on the E-box, as suggested by previous studies (13, 17, 18). Our results support a recent study showing that the stoichiometry of the PER–CRY complex is important for the proper displacement of CLOCK–BMAL1 from the E-box (61). Several studies suggested that both CRYs and PERs have a nuclear localization signal for their translocation into the nucleus to be able to perform transcriptional feedback function (62–64). In addition, CRY2 interacts with the importin alpha/beta system through a bipartite nuclear localization signal in its carboxyl end, allowing the translocation of CRY2 along with PER2 into the cell nucleus (65). However, another study indicated that a CRY2 double mutant, which is incapable of interacting with PER2, can move into the nucleus (51).

Overall, the results of this study indicate that Pro123Leu, Asp406His, and Ser410Ile mutations located at the secondary pocket rim have functional effects on the repressor activity of CRY2 through improper nuclear localization. Although they have not yet been related to any diseases, this study suggests that these variants should also be taken into consideration, especially in circadian-related diseases like sleep disorders, hormonal and neural defects, and depression. Further *in vivo* studies are required to understand their contribution to disease etiology.

Experimental procedures

SDM

Phusion polymerase based quick-change mutagenesis was used for single nucleotide change. SDM was performed on pcDNA-*Cry2*-Myc-His and on pMU2-P(CRY1)-(intron 336)-Cry2 for three variants using the primers in Table S1. The PCR mixtures contained 1× HF buffer, 200 μM dNTP mix, 0.3 μM forward and reverse primers, 50 ng of the template plasmid, and 1 unit of Phusion Hot Start Flex DNA Polymerase (NEB; catalog no.: M0535S) in a 50 μl of final volume. The reaction conditions were set to 98 °C for 30 s, 62 °C for 30 s, and 72 °C for 10 min, 29 cycles. PCR products were visualized in 0.8% agarose gel. The samples with correct sized bands were digested with 1 unit of FastDigest DpnI enzyme (Thermo Fisher Scientific; catalog no.: FD1703) for 1 h at 37 °C, and then 7 μl of sample was transformed to TOP10 *Escherichia coli* cells. Colonies were picked to culture, and then plasmids were isolated with Nucleospin Plasmid kit (Macherey–Nagel; catalog no.: 740588.50) using the manufacturer's instruction. Sanger sequencing (Macrogen) was used to confirm the mutations.

Repression assay of CLOCK–BMAL1–dependent transactivation

HEK293T cells (4×10^4) were transfected with polyethyleneimine (PEI) (Polysciences; catalog no.: 23966-1) transfection reagent with the following amount of plasmids in a 96-well opaque plate by reverse transfection: 25 ng of pCMV-Sport6-*CLOCK*, 50 ng of pCMV-Sport6-*Bmal1*, 50 ng of pGL3-*mPer1*:d*Luc* marker, 20 ng of pFLAG-CMV-*Per2*, and dose-dependent manner of WT and Cry2 variant plasmids. pcDNA-empty was used to equalize transfected plasmid concentration. To determine the activity of CLOCK–BMAL1–dependent transactivation without a repressor, the mixture was supplemented with empty pcDNA4/myc-His A instead of *Cry2* construct. In each independent experiment, transfections were triplicated for each condition. After 24 h of incubation in humidified cell incubator supplemented with 5% CO_2, cells were lysed with Firefly luciferase. Firefly luciferase activity was measured with Fluoroskan Ascent FL microplate reader.

Measurements were normalized with Renilla luciferase expression with the same protocol but using Renilla buffer.

Extraction of proteins from cells and Western blotting

The cells are harvested with ice-cold PBS solution (137 mM NaCl, 2.7 mM KCl, 10 mM Na_2HPO_4, 1.8 mM KH_2PO_4, pH 7.4) and centrifuged at 4000*g* for 5 min. PBS was vacuumed, and the cell pellet was kept at −20 °C. The pellet was resuspended in ice-cold radioimmunoprecipitation assay buffer (150 mM NaCl, 50 mM Tris, 0.1% SDS, 1% Triton-X, 1% protease inhibitor cocktail) (PIC; catalog no.: 78430). After 20 min of incubation on ice, lysed cells were centrifugated at 15,000*g* for 20 min at +4 °C, and supernatants were transferred to a new Eppendorf tube. To measure total protein concentration, Pierce assay (Thermo Fisher Scientific; catalog no.: 22660) was used according to the manufacturer's manual. Measurements were taken by Epoch microplate reader at 660 nm. Afterward, 4× Laemmli buffer (250 mM Tris–HCl at pH 6.8, 40% glycerol, 4% SDS, 0.02% bromophenol blue, and 10% β-mercaptoethanol, which is freshly added) was used as sample buffer for SDS-PAGE. After adding 4× Laemmli buffer, samples were boiled at 95 °C for 10 min. For Western blotting, total protein samples were subjected to SDS-PAGE; for stacking, 5% gel was used, whereas for separating 10% gel was used. The proteins were transferred to polyvinylidene fluoride membrane (Millipore; catalog no.: IEVH00005) by wet Western blot transfer. A sandwich was prepared in the order of sponge, Whatman paper, gel, polyvinylidene fluoride membrane, Whatman paper, and sponge. The sandwich located in the tank, where the gel was facing to the negative electrode, was filled with Western blot transfer buffer (3.04 g Tris base, 14.4 g glycine, 200 ml methanol, ddH_2O up to 1 l). Membrane was blocked with 5% milk solution in 0.15% Tris-buffered saline (TBS)–Tween-20 for 1 h and then incubated overnight with the following primary antibodies where they are necessary: anti-FLAG (Sigma–Aldrich; catalog no.: SAB4200071), anti-Myc (Abcam; catalog no.: ab18185), anti-β-actin (Cell Signalling; catalog no.: 4970), anti-Histone H3 antibody (Abcam; catalog no.: ab1791), and monoclonal anti-α-tubulin antibody (Sigma–Aldrich; T9026). After washing membranes with three times for 5 min with 0.15% TBS–Tween, membranes were incubated 1 h with appropriate horseradish peroxidase (HRP)–conjugated antimouse (Santa Cruz; catalog no.: SC-358920), HRP-conjugated anti-rabbit (Cell Signaling; catalog no.: 7074), rabbit polyclonal immunoglobulin G (Santa Cruz; catalog no.: sc-48805) secondary antibodies. Before imaging, the membrane was again washed with TBS-T three times for 5 min. For the imaging process, the homemade ECL buffer was prepared freshly (1.25 mM luminol, 0.225 mM *p*-coumeric acid, 0.1 M Tris (pH = 8.8), H_2O_2 (9×10^{-5} [v/v]), and the membrane was incubated in it for 4 min. Images were taken and quantified by Bio-Rad Chemidoc.

Protein complex immunoprecipitation

About 3.2×10^5 HEK293T cells/well were seeded in a 6-well plate, 24 h before the transfection. Cells are transfected with 500 ng pcDNA4/myc-His-A-*Cry2* (WT or variants), 350 ng pFLAG-CMV-*Per2*, 150 ng pFLAG-CMV-*CLOCK*, and 1000 ng pFLAG-CMV-*Bmal1 via* PEI transfection reagent. Plasmids containing *Bmal1*, *CLOCK*, and *Per2* cDNAs were transfected with empty pCMV-Sport6 instead as negative control. After 24 h of incubation, the cells were harvested as it was explained in the "Extraction of proteins from cells and Western blotting" section.

After harvesting the cells with centrifugation, cell pellets were resuspended in passive lysis buffer (PLB) (15 mM Hepes, 5 mM NaF, 300 mM NaCl, 1% NP-40, and 1% PIC) and were incubated on ice for 20 min. Lysates were centrifugated at 15,000*g* for 20 min at +4 °C, and supernatants were taken to a new Eppendorf tube. About 10% of the supernatant was saved as input. EZview Red Anti-c-Myc Affinity Gel beads (catalog no.: E6654) were equilibrated by PLB two times. Supernatants from the cell lysates were transferred on the equilibrated beads, and samples were rotated in a vertical rotator at +4 °C for 2 h. Samples were centrifugated for 30 s at 8200*g*. Supernatants were removed. Beads were washed by adding PLB without PIC rotating at +4 °C for 5 min. The washing steps were repeated two more times. After removing the final wash supernatant, proteins were isolated from resins by boiling in Laemmli buffer (250 mM Tris–HCl [pH 6.8], 40% glycerol, 4% SDS, 0.02% bromophenol blue, and 10% freshly added β-mercaptoethanol). Western blotting was performed as described with anti-FLAG antibody (Sigma; catalog no.: A9469), used to detect BMAL1, CLOCK, and PER2. Blots were stripped (Advansta strip-it buffer [R03722-D50]) and incubated with anti-Myc antibody (abcam; catalog no.: ab18185) to detect CRY2. HRP-conjugated antimouse (Santa Cruz Biotechnology; catalog no.: 516102) was used as the secondary antibody.

Real-time bioluminescence rescue assay

MEF $Cry1^{-/-}Cry2^{-/-}$ (DKO-MEF) cell lines (gifted by Prof Ueda, RIKEN, Japan). About 3.2×10^5 DKO-MEF cells were seeded into 35 mm culture dishes. pGL3-*Per2*-dLuc (luciferase reporter, 4000 ng) and pMU2-P(CRY1)-(intron 336)-Cry2 (WT or variants, 150 ng, 900 ng) were transfected by using FuGENE6 transfection reagent (Promega; catalog no.: E2691) 24 h after seeding. After 72 h of incubation, the cells were synchronized with dexamethasone (Sigma–Aldrich; catalog no.: D4902) with a final concentration of 0.1 μM. After 2 h of incubation, the medium was replaced with bioluminescence recording media, which contains the following in 1 l: Dulbecco's modified Eagle's medium powder (Sigma; catalog no.: D-2902; 10× 1 l), 0.35 g sodium bicarbonate (tissue culture grade; Sigma; catalog no.: S5761), 3.5 g D(+) glucose powder (tissue culture grade; Sigma; catalog no.: G7021), 10 ml 1 M Hepes buffer (Gibco; catalog no.: 15140-122), 2.5 ml penicillin/streptomycin (100 μg/ml), 50 ml 5% fetal bovine serum, and up to 1 l sterile milliQ water. The plates were sealed with silicon grease and were placed into LumiCycle 32 Luminometer (Actimetrics). Bioluminescence recordings were taken with a photomultiplier for 70 s every 10 min for 5 days.

The role of the secondary pocket in CRY2 activity

Protein degradation assays

About 2.25 × 10^5 HEK293T cells/well were seeded to a 12-well tissue culture plate. pcDNA4/myc-His-A-*Cry2* (WT or variants, 500 ng) and pSG5-*Per2*-FLAG (500 ng) plasmids were transfected *via* PEI transfection reagent. After 24 h, cells were treated with CHX (Sigma; catalog no.: 66819) with a final concentration of 20 μg/ml. Cells were harvested at 4 h intervals up to the 12th hour. Cells that were collected right after CHX treatment were marked as t = 0 h. Protein amounts were detected by Western blotting using anti-Myc and anti-β-actin. The detailed protocol was explained in the "Extraction of proteins from cells and Western blotting" section. In addition, to test the effect of inhibition of the proteasome degradation, the cells are treated with CHX (20 μg/ml) plus MG132 (Sigma; catalog no.: 1211877-36-9) with final concentration of 10 μM. Cells were harvested, and the protein was detected with the same protocol.

Subcellular fractionations of the WT and CRY2 variants

About 5 × 10^5HEK293T cells/well were seeded to a 6-well plate. After 24 h, cells were transfected with 500 ng pcDNA4/myc-His-*Cry2* (WT or variants) and 500 ng pSG-*Per2*-FLAG via PEI transfection reagent. After 24 h of incubation, the cells were harvested and lysed with cytosolic lysis buffer (10 mM Hepes [pH 7.9], 10 mM KCl, 0.1 mM EDTA, 0.05% NP-40, and proteasome inhibitor). Then samples were incubated 10 min on ice and centrifuged for 5 min at 650*g* at 4 °C. The supernatant was saved as the cytosolic fraction, and pellets were processed for the nuclear fraction. The nuclear fraction was washed with cytosolic lysis buffer and centrifuged for 5 min at 650*g* at 4 °C, two times. The pellet was dissolved in nuclear lysis buffer (20 mM Hepes [pH 7.9], 0.4 M NaCl, 1 mM EDTA, 10% glycerol, and protease inhibitor), sonicated (60% power, 10 s × 3 cycles) and centrifuged 15,000*g* for 5 min at 4 °C, and the supernatant was saved as the nuclear fraction. The cytosolic fraction was also centrifuged at 15,000*g* for 5 min at 4 °C, the cell debris was removed in the pellet, and the supernatant was saved as the cytosolic fraction. After determining the protein amount, the fractions were supplemented with Laemmli buffer, and Western blotting was performed as described in the "Extraction of proteins from cells and Western blotting" section.

Data availability

All data generated or analyzed during this study are included in this article and its supporting information files.

Supporting information—This article contains supporting information.

Acknowledgments—This work is supported by TUBITAK-KBAG 121Z862.

Author contributions—G. C. P., B. B. C., I. B., O. O., S. G., and I. H. K. methodology; G. C. P., B. B. C., S. G., and O. O. formal analysis; G. C. P., B. B. C., S. G., and O. O. investigation; G. C. P., B. B. C., S. G., O. O., I. B., and I. H. K. writing–original draft; I.H.K. supervision; I.H.K. funding acquisition.

Conflict of interest—The authors declare that they have no conflicts of interest with the contents of this article.

Abbreviations—The abbreviations used are: β-TrCP1, β-transducin repeat–containing protein 1; BMAL1, brain and muscle ARNT-like-1; cDNA, complementary DNA; CHX, cycloheximide; CLOCK, circadian locomotor output cycles kaput; co-IP, coimmunoprecipitation; CRY2, cryptochrome 2; DKO, double KO; FBXL3, F-box and leucine-rich repeat protein 3; HEK293T, human embryonic kidney 293T cell line; HRP, horseradish peroxidase; MEF, mouse embryonic fibroblast; PEI, polyethyleneimine; PER, period; PH, photolyase homology; PIC, protease inhibitor cocktail; PLB, passive lysis buffer; SDM, site-directed mutagenesis; TBS, Tris-buffered saline; TTFL, transcriptional–translational feedback loop.

References

1. Kavakli, I. H., Gul, S., and Turkay, M. (2022) Identification of novel small molecules targeting core clock proteins to regulate circadian rhythm. *Curr. Opin. Chem. Eng.* **35**, 100730
2. Lowrey, P. L., and Takahashi, J. S. (2011) Genetics of circadian rhythms in mammalian model organisms. *Adv. Genet.* **74**, 175–230
3. Kavakli, I. H., and Sancar, A. (2002) Circadian photoreception in humans and mice. *Mol. Interv.* **2**, 484–492
4. Panda, S., Antoch, M. P., Miller, B. H., Su, A. I., Schook, A. B., Straume, M., *et al.* (2002) Coordinated transcription of key pathways in the mouse by the circadian clock. *Cell* **109**, 307–320
5. Takahashi, J. S. (2017) Transcriptional architecture of the mammalian circadian clock. *Nat. Rev. Genet.* **18**, 164–179
6. Kavakli, I. H., Ozturk, N., and Baris, I. (2022) Protein interaction networks of the mammalian core clock proteins. *Adv. Protein Chem. Struct. Biol.* **131**, 207–233
7. Allada, R., and Bass, J. (2021) Circadian mechanisms in medicine. *N. Engl. J. Med.* **384**, 550–561
8. Sherman, B., Wysham, C., and Pfohl, B. (1985) Age-related changes in the circadian rhythm of plasma cortisol in man. *J. Clin. Endocrinol. Metab.* **61**, 439–443
9. Vitaterna, M. H., Selby, C. P., Todo, T., Niwa, H., Thompson, C., Fruechte, E. M., *et al.* (1999) Differential regulation of mammalian period genes and circadian rhythmicity by cryptochromes 1 and 2. *Proc. Natl. Acad. Sci. U. S. A.* **96**, 12114–12119
10. Reischl, S., Vanselow, K., Westermark, P. O., Thierfelder, N., Maier, B., Herzel, H., *et al.* (2007) beta-TrCP1-mediated degradation of PERIOD2 is essential for circadian dynamics. *J. Biol. Rhythms* **22**, 375–386
11. Siepka, S. M., Yoo, S. H., Park, J., Song, W., Kumar, V., Hu, Y., *et al.* (2007) Circadian mutant overtime reveals F-box protein FBXL3 regulation of cryptochrome and period gene expression. *Cell* **129**, 1011–1023
12. Takahashi, J. S. (2016) Molecular architecture of the circadian clock in mammals. In: Sassone-Corsi, P., Christen, Y., eds. *A Time for Metabolism and Hormones*, Springer, Cham, Switzerland: 13–24
13. Ye, R., Selby, C. P., Chiou, Y. Y., Ozkan-Dagliyan, I., Gaddameedhi, S., and Sancar, A. (2014) Dual modes of CLOCK:BMAL1 inhibition mediated by cryptochrome and period proteins in the mammalian circadian clock. *Genes Dev.* **28**, 1989–1998
14. Etchegaray, J. P., Lee, C., Wade, P. A., and Reppert, S. M. (2003) Rhythmic histone acetylation underlies transcription in the mammalian circadian clock. *Nature* **421**, 177–182
15. Kume, K., Zylka, M. J., Sriram, S., Shearman, L. P., Weaver, D. R., Jin, X., *et al.* (1999) mCRY1 and mCRY2 are essential components of the negative limb of the circadian clock feedback loop. *Cell* **98**, 193–205
16. Shearman, L. P., Jin, X., Lee, C., Reppert, S. M., and Weaver, D. R. (2000) Targeted disruption of the mPer3 gene: subtle effects on circadian clock function. *Mol. Cell. Biol.* **20**, 6269–6275

17. Ye, R., Selby, C. P., Ozturk, N., Annayev, Y., and Sancar, A. (2011) Biochemical analysis of the canonical model for the mammalian circadian clock. *J. Biol. Chem.* **286**, 25891–25902
18. Cao, X., Yang, Y., Selby, C. P., Liu, Z., and Sancar, A. (2021) Molecular mechanism of the repressive phase of the mammalian circadian clock. *Proc. Natl. Acad. Sci. U. S. A.* **118**, e2021174118
19. Kavakli, I. H., Baris, I., Tardu, M., Gul, S., Oner, H., Cal, S., *et al.* (2017) The photolyase/cryptochrome family of proteins as DNA repair enzymes and transcriptional repressors. *Photochem. Photobiol.* **93**, 93–103
20. Partch, C. L., Clarkson, M. W., Ozgur, S., Lee, A. L., and Sancar, A. (2005) Role of structural plasticity in signal transduction by the cryptochrome blue-light photoreceptor. *Biochemistry* **44**, 3795–3805
21. Sancar, A. (2003) Structure and function of DNA photolyase and cryptochrome blue-light photoreceptors. *Chem. Rev.* **103**, 2203–2237
22. Gao, P., Yoo, S. H., Lee, K. J., Rosensweig, C., Takahashi, J. S., Chen, B. P., *et al.* (2013) Phosphorylation of the cryptochrome 1 C-terminal tail regulates circadian period length. *J. Biol. Chem.* **288**, 35277–35286
23. Khan, S. K., Xu, H., Ukai-Tadenuma, M., Burton, B., Wang, Y., Ueda, H. R., *et al.* (2012) Identification of a novel cryptochrome differentiating domain required for feedback repression in circadian clock function. *J. Biol. Chem.* **287**, 25917–25926
24. Cal-Kayitmazbatir, S., Kulkoyluoglu-Cotul, E., Growe, J., Selby, C. P., Rhoades, S. D., Malik, D., *et al.* (2021) CRY1-CBS binding regulates circadian clock function and metabolism. *FEBS J.* **288**, 614–639
25. Michael, A. K., Fribourgh, J. L., Chelliah, Y., Sandate, C. R., Hura, G. L., Schneidman-Duhovny, D., *et al.* (2017) Formation of a repressive complex in the mammalian circadian clock is mediated by the secondary pocket of CRY1. *Proc. Natl. Acad. Sci. U. S. A.* **114**, 1560–1565
26. Fribourgh, J. L., Srivastava, A., Sandate, C. R., Michael, A. K., Hsu, P. L., Rakers, C., *et al.* (2020) Dynamics at the serine loop underlie differential affinity of cryptochromes for CLOCK:BMAL1 to control circadian timing. *Elife* **9**, e55275
27. Gul, S., Aydin, C., Ozcan, O., Gurkan, B., Surme, S., Baris, I., *et al.* (2020) The Arg-293 of Cryptochrome1 is responsible for the allosteric regulation of CLOCK-CRY1 binding in circadian rhythm. *J. Biol. Chem.* **295**, 17187–17199
28. Ozcan, O., Gul, S., and Kavakli, I. H. (2021) Allosteric regulation of CRYs in mammalian circadian clock. In: Turkay, M., Gani, R., eds.**, Vol. 50**. *Computer Aided Chemical Engineering*, Elsevier, Netherlands: 2025–2031
29. Hirano, A., Shi, G., Jones, C. R., Lipzen, A., Pennacchio, L. A., Xu, Y., *et al.* (2016) A cryptochrome 2 mutation yields advanced sleep phase in humans. *Elife* **5**, e16695
30. Lavebratt, C., Sjoholm, L. K., Soronen, P., Paunio, T., Vawter, M. P., Bunney, W. E., *et al.* (2010) CRY2 is associated with depression. *PLoS One* **5**, e9407
31. Liu, C., Li, H., Qi, L., Loos, R. J., Qi, Q., Lu, L., *et al.* (2011) Variants in GLIS3 and CRY2 are associated with type 2 diabetes and impaired fasting glucose in Chinese Hans. *PLoS One* **6**, e21464
32. Onat, O. E., Kars, M. E., Gul, S., Bilguvar, K., Wu, Y., Ozhan, A., *et al.* (2020) Human CRY1 variants associate with attention deficit/hyperactivity disorder. *J. Clin. Invest.* **130**, 3885–3900
33. Patke, A., Murphy, P. J., Onat, O. E., Krieger, A. C., Özçelik, T., Campbell, S. S., *et al.* (2017) Mutation of the human circadian clock gene CRY1 in familial delayed sleep phase disorder. *Cell* **169**, 203–215.e3
34. Chen, Z., Yoo, S.-H., and Takahashi, J. S. (2018) Development and therapeutic potential of small-molecule modulators of circadian systems. *Annu. Rev. Pharmacol. Toxicol.* **58**, 231–252
35. Doruk, Y. U., Yarparvar, D., Akyel, Y. K., Gul, S., Taskin, A. C., Yilmaz, F., *et al.* (2020) A CLOCK-binding small molecule disrupts the interaction between CLOCK and BMAL1 and enhances circadian rhythm amplitude. *J. Biol. Chem.* **295**, 3518–3531
36. [preprint] Gul, S., Akyel, Y. K., Gul, Z. M., Isin, S., Korkmaz, T., Selvi, S., *et al.* (2021) Discovery of a small molecule that selectively destabilizes cryptochrome 1 and enhances life span in p53 knockout mice. *bioRxiv*. https://doi.org/10.1101/2021.07.21.453206
37. Gul, S., Rahim, F., Isin, S., Yilmaz, F., Ozturk, N., Turkay, M., *et al.* (2021) Structure-based design and classifications of small molecules regulating the circadian rhythm period. *Sci. Rep.* **11**, 18510
38. Hirota, T., Lee, J. W., St John, P. C., Sawa, M., Iwaisako, K., Noguchi, T., *et al.* (2012) Identification of small molecule activators of cryptochrome. *Science* **337**, 1094–1097
39. Genomes Project, C., Auton, A., Brooks, L. D., Durbin, R. M., Garrison, E. P., Kang, H. M., *et al.* (2015) A global reference for human genetic variation. *Nature* **526**, 68–74
40. Zerbino, D. R., Achuthan, P., Akanni, W., Amode, M. R., Barrell, D., Bhai, J., *et al.* (2018) Ensembl 2018. *Nucleic Acids Res.* **46**, D754–D761
41. Schwarz, J. M., Cooper, D. N., Schuelke, M., and Seelow, D. (2014) MutationTaster2: mutation prediction for the deep-sequencing age. *Nat. Methods* **11**, 361–362
42. Richards, S., Aziz, N., Bale, S., Bick, D., Das, S., Gastier-Foster, J., *et al.* (2015) Standards and guidelines for the interpretation of sequence variants: a joint consensus recommendation of the American College of Medical Genetics and Genomics and the Association for Molecular Pathology. *Genet. Med.* **17**, 405–424
43. Adzhubei, I. A., Schmidt, S., Peshkin, L., Ramensky, V. E., Gerasimova, A., Bork, P., *et al.* (2010) A method and server for predicting damaging missense mutations. *Nat. Methods* **7**, 248–249
44. Ioannidis, N. M., Rothstein, J. H., Pejaver, V., Middha, S., McDonnell, S. K., Baheti, S., *et al.* (2016) REVEL: an ensemble method for predicting the pathogenicity of rare missense variants. *Am. J. Hum. Genet.* **99**, 877–885
45. Ng, P. C., and Henikoff, S. (2003) SIFT: predicting amino acid changes that affect protein function. *Nucleic Acids Res.* **31**, 3812–3814
46. Kircher, M., Witten, D. M., Jain, P., O'Roak, B. J., Cooper, G. M., and Shendure, J. (2014) A general framework for estimating the relative pathogenicity of human genetic variants. *Nat. Genet.* **46**, 310–315
47. Reva, B., Antipin, Y., and Sander, C. (2011) Predicting the functional impact of protein mutations: application to cancer genomics. *Nucleic Acids Res.* **39**, e118
48. Rosensweig, C., and Green, C. B. (2020) Periodicity, repression, and the molecular architecture of the mammalian circadian clock. *Eur. J. Neurosci.* **51**, 139–165
49. Rosensweig, C., Reynolds, K. A., Gao, P., Laothamatas, I., Shan, Y., Ranganathan, R., *et al.* (2018) An evolutionary hotspot defines functional differences between CRYPTOCHROMES. *Nat. Commun.* **9**, 1138
50. Miki, T., Matsumoto, T., Zhao, Z., and Lee, C. C. (2013) p53 regulates Period2 expression and the circadian clock. *Nat. Commun.* **4**, 2444
51. Ozber, N., Baris, I., Tatlici, G., Gur, I., Kilinc, S., Unal, E. B., *et al.* (2010) Identification of two amino acids in the C-terminal domain of mouse CRY2 essential for PER2 interaction. *BMC Mol. Biol.* **11**, 69
52. Nangle, S., Xing, W., and Zheng, N. (2013) Crystal structure of mammalian cryptochrome in complex with a small molecule competitor of its ubiquitin ligase. *Cell Res.* **23**, 1417–1419
53. Eide, E. J., Woolf, M. F., Kang, H., Woolf, P., Hurst, W., Camacho, F., *et al.* (2005) Control of mammalian circadian rhythm by CKIepsilon-regulated proteasome-mediated PER2 degradation. *Mol. Cell. Biol.* **25**, 2795–2807
54. Kao, S. H., Wang, W. L., Chen, C. Y., Chang, Y. L., Wu, Y. Y., Wang, Y. T., *et al.* (2015) Analysis of protein stability by the cycloheximide chase assay. *Bio Protoc.* **5**, e1374
55. Busino, L., Bassermann, F., Maiolica, A., Lee, C., Nolan, P. M., Godinho, S. I., *et al.* (2007) SCFFbxl3 controls the oscillation of the circadian clock by directing the degradation of cryptochrome proteins. *Science* **316**, 900–904
56. Godinho, S. I., Maywood, E. S., Shaw, L., Tucci, V., Barnard, A. R., Busino, L., *et al.* (2007) The after-hours mutant reveals a role for Fbxl3 in determining mammalian circadian period. *Science* **316**, 897–900
57. Hirano, A., Yumimoto, K., Tsunematsu, R., Matsumoto, M., Oyama, M., Kozuka-Hata, H., *et al.* (2013) FBXL21 regulates oscillation of the circadian clock through ubiquitination and stabilization of cryptochromes. *Cell* **152**, 1106–1118
58. Yoo, S. H., Mohawk, J. A., Siepka, S. M., Shan, Y., Huh, S. K., Hong, H. K., *et al.* (2013) Competing E3 ubiquitin ligases govern circadian periodicity by degradation of CRY in nucleus and cytoplasm. *Cell* **152**, 1091–1105

59. Ukai-Tadenuma, M., Yamada, R. G., Xu, H. Y., Ripperger, J. A., Liu, A. C., and Ueda, H. R. (2011) Delay in feedback repression by cryptochrome 1 is required for circadian clock function. *Cell* **144**, 268–281
60. Schmalen, I., Reischl, S., Wallach, T., Klemz, R., Grudziecki, A., Prabu, J. R., *et al.* (2014) Interaction of circadian clock proteins CRY1 and PER2 is modulated by zinc binding and disulfide bond formation. *Cell* **157**, 1203–1215
61. Koch, A. A., Bagnall, J. S., Smyllie, N. J., Begley, N., Adamson, A. D., Fribourgh, J. L., *et al.* (2022) Quantification of protein abundance and interaction defines a mechanism for operation of the circadian clock. *Elife* **11**, e73976
62. Hirayama, J., Nakamura, H., Ishikawa, T., Kobayashi, Y., and Todo, T. (2003) Functional and structural analyses of cryptochrome. Vertebrate CRY regions responsible for interaction with the CLOCK:BMAL1 heterodimer and its nuclear localization. *J. Biol. Chem.* **278**, 35620–35628
63. Miyazaki, K., Mesaki, M., and Ishida, N. (2001) Nuclear entry mechanism of rat PER2 (rPER2): role of rPER2 in nuclear localization of CRY protein. *Mol. Cell. Biol.* **21**, 6651–6659
64. Vielhaber, E. L., Duricka, D., Ullman, K. S., and Virshup, D. M. (2001) Nuclear export of mammalian PERIOD proteins. *J. Biol. Chem.* **276**, 45921–45927
65. Sakakida, Y., Miyamoto, Y., Nagoshi, E., Akashi, M., Nakamura, T. J., Mamine, T., *et al.* (2005) Importin alpha/beta mediates nuclear transport of a mammalian circadian clock component, mCRY2, together with mPER2, through a bipartite nuclear localization signal. *J. Biol. Chem.* **280**, 13272–13278